

See discussions, stats, and author profiles for this publication at: <https://www.researchgate.net/publication/256707095>

Effect of Rotational Degrees of Freedom on Molecular Mobility

ARTICLE *in* THE JOURNAL OF PHYSICAL CHEMISTRY C · MARCH 2013

Impact Factor: 4.77 · DOI: 10.1021/jp312438u

CITATIONS

5

READS

44

3 AUTHORS, INCLUDING:



[Mehdi Jafary-Zadeh](#)

Institute Of High Performance Computing

11 PUBLICATIONS 36 CITATIONS

[SEE PROFILE](#)



[Chilla Damodara Reddy](#)

Institute Of High Performance Computing

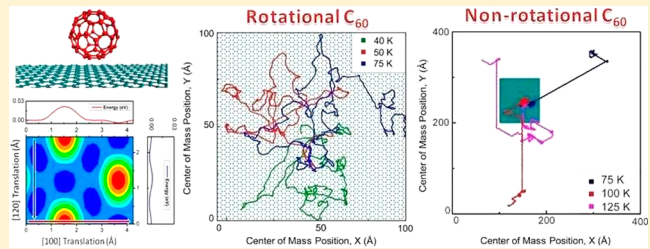
32 PUBLICATIONS 670 CITATIONS

[SEE PROFILE](#)

Effect of Rotational Degrees of Freedom on Molecular Mobility

M. Jafary-Zadeh,[†] C. D. Reddy,[‡] and Yong-Wei Zhang^{*‡}[†]Department of Materials Science and Engineering, National University of Singapore, Singapore 119260[‡]Institute of High Performance Computing, A*STAR, Singapore 138632

ABSTRACT: A molecule is a basic building block in bottom-up approach to develop nanoscale machinery and electro-mechanical systems. Because of finite size and rotational degrees of freedom (DOFs), its diffusion behavior is generally more complex than its atomic counterpart. Understanding the effect of rotational DOFs on molecular diffusion is not only important for controlling molecular motion but also essential for many device applications. Here, we use molecular dynamics simulations to study the effect of rotational DOFs on the surface diffusion of C_{60} on graphene substrate. We show that there is an intermediate temperature range in which the rotational DOFs play a pronounced role in enhancing the molecular mobility in the system, which is in contrast to both the low- and high-temperature regimes in which the rotational DOFs show little influence. We further analyze the underlying mechanistic origin for the enhancement and find that in this regime the rotational DOFs provide alternative routes for the admolecule to overcome the energy barriers of the system, leading to a quasi-continuous Brownian motion on the surface. Our results provide new insights into molecular surface diffusion.



INTRODUCTION

Molecules, nanoparticles, and nanoclusters, which are shown to exhibit various fascinating structural, electronic, magnetic, and optical properties, are the basic building blocks for constructing functional structures and nanodevices.^{1–3} Under thermal activation and/or external fields, these nanoscale building blocks are often required to perform specified movements. How to precisely control their motion so as to achieve the prescribed trajectory or mobility is, however, a current ongoing research topic.^{4–6} In contrast to adatom, these building blocks have rotational degrees of freedom (DOFs) and occupy a finite space, whose dimensions are generally larger than the interatomic spacing. As a consequence, their diffusion behavior is more complex than their atomic counterpart.^{7,8} Hence, understanding the effect of rotational DOFs of these basic building blocks on their diffusion behavior is not only important to control molecular motion but also essential for many applications such as nanotribology,⁹ molecular machinery, and nanoelectromechanical systems (NEMS).¹⁰

The diffusive behavior of a molecule (nanoparticle or nanocluster) on a substrate is fundamental in many practical applications. The complexity of molecular surface diffusion raises questions in using existing atomic diffusion theories to interpret molecular diffusion.⁷ The conventional and widely used model of surface diffusion is based on the transition state theory (TST), which describes the diffusion of an adsorbate as the result of a series of thermally activated and uncorrelated random jumps (hopping) between adjacent adsorption sites,¹¹ and the diffusion process is primarily controlled by the profile (shape) of the potential energy surface (PES) of the system.^{11,12} Recognizing the importance of rotational DOFs of nanoscale building blocks, several studies were performed to understand their effect on the

diffusion and friction mechanisms.^{10,13–17} For example, theoretical studies^{18–20} showed that even in the simplest case of rigid molecule consisting of only two or three atoms, rotational DOFs can enhance the surface diffusion rate. Molecular dynamics (MD) studies²¹ indicated that the energy barrier of lateral diffusion of an admolecule can be overcome by changing the configuration or orientation of the admolecule. MD simulations²² also revealed that in the absence of rotational DOFs, a benzene molecule performs stick-slip motion, which is accompanied by frequent occurrence of long jumps (flights) on a graphite substrate. The correlation between rotation and translation of adsorbed nanoclusters has been reported in different regimes of motion (diffusive and ballistic).⁹ Despite all theoretical and experimental efforts, several important questions regarding molecular diffusion remain unanswered: (1) How do the rotational DOFs affect the diffusion regimes? (2) What is the role of rotational DOFs in the interaction between an admolecule and substrate? (3) How is the effect of rotational DOFs on the mobility of admolecule in each regime quantified?

Motivated by the intriguing questions discussed above, we chose C₆₀/graphene as a model system to study the effect of rotational DOFs of the C₆₀ molecule on its diffusive behavior on graphene. It is noted that organic molecules adsorbed on graphene are important in exploiting graphene for many technological applications.^{23,24} For example, the van der Waals epitaxy of C₆₀ on graphene was recently realized^{25,26} and envisioned for many potential applications such as molecular bearings,²⁷ spintronics, and quantum computing.^{26,28} In

Received: December 18, 2012

Revised: March 4, 2013

Published: March 13, 2013

addition, it was shown that the rotation of C_{60} molecule plays an important role in achieving ultralow static friction at the graphite/ C_{60} /graphite interface.²⁹ Owing to its spherical shape and rotational DOFs, C_{60} could serve as an ideal wheel for rolling motion on surface.³⁰ Moreover, the application of C_{60} for drug and gene delivery was also envisioned in a biomedical field.^{31,32} These promising applications indicate the importance of understanding the motion of C_{60} molecule in various environments, including on surface and membrane.^{33–35} Hence, the physisorbed C_{60} /graphene is an ideal system for investigating the role of rotational DOFs in molecular surface diffusion.

In the present work, we perform systematic simulations of the C_{60} /graphene system in a wide range of temperature and in the presence and absence of C_{60} rotational DOFs. We then analyze and compare the resulting diffusive regimes and their corresponding mobilities. Our goal is to address the issues raised above, that is, how C_{60} rotational DOFs affect its surface diffusion regimes and their corresponding mobilities.

METHODS AND MODEL

The computational model consists of a single C_{60} admolecule and a graphene substrate. The molecular dynamics (MD) simulations were performed at temperatures between 5 and 200 K using Large-scale Atomic/Molecular Massively Parallel Simulator (LAMMPS)³⁶ and the Adaptive Intermolecular Reactive Empirical Bond Order (AIREBO) potential.³⁷ This potential is one of the most successful potentials and has been applied to model both chemical reactions and intermolecular interactions in hydrocarbon systems including graphene.³⁸

Periodic boundary conditions (PBC) were applied along the in-plane directions of the graphene substrate with dimensions of 50 Å by 50 Å, which represents an infinite surface. The C_{60} molecule was positioned at equilibrium distance of 3.1 Å on the top of the substrate in such a way that one of its hexagon faces was initially oriented parallel to the graphene substrate. Here, this configuration is referred to as “hexagon in phase” (Hex-In Phase). In order to study the dynamics of the system, the microcanonical ensemble was selected. At the beginning of each simulation, energy minimization was performed to relax the atomic positions of the system using the Polak–Ribiere conjugate gradient (CG) method. After energy minimization, the velocities of the atoms in the system were assigned following the Maxwell–Boltzmann distribution at the desired temperature in such a way that no initial aggregate linear and angular momenta were imposed on the system. Each trajectory calculation was started with a 50 ps thermal equilibration, followed by a run of up to 20 ns to extract data for diffusion analysis. The time step of the Verlet integration algorithm was set to be 1 fs.

The trajectories of the C_{60} center of mass (COM) at different temperatures were obtained from the simulations. At a sufficiently long time scale, the mean-square displacement (MSD) of the C_{60} COM scales linearly with time and the diffusion coefficient, D , and can be calculated using the best linear fit to the MSD curves according to

$$\text{MSD} = \langle \Delta r^2(t) \rangle = 2dDt \quad (1)$$

where Δr is the displacement of the admolecule COM with respect to the origin, t is the time, $\langle \rangle$ denotes time or ensemble average, and d is the dimensionality of the system, which is equal to 2 for the surface diffusion problems. To have a better statistics, the MSD curves were calculated using multiple time origin

technique^{39–41} (400 time origins were used), and the long time simulations were repeated up to five times.

Based on the MD technique used in the current work, all degrees of freedom of the system, including the C_{60} rotational DOFs, were explicitly taken into account. In order to study the effect of rotational DOFs on the dynamics of surface diffusion and mobility of C_{60} , a second series of simulations were also performed at the same temperature range, in which, however, the rotational DOFs of the C_{60} were frozen based on the energy separation technique and routines provided by the LAMMPS package.^{36,42–44} It is noteworthy that in these simulations only the rotational DOFs of C_{60} were frozen while all its other DOFs were remained untouched. The results of two different sets of simulations (in the presence and absence of C_{60} rotation) were analyzed and compared with each other to examine the effect of rotational DOFs on the surface diffusion of the C_{60} admolecule. For simplicity, hereafter, the C_{60} admolecule in the presence and absence of rotational DOFs is referred to as R- C_{60} and NR- C_{60} , respectively.

RESULTS AND DISCUSSION

The simulations were performed to identify and characterize different diffusion regimes in both R- C_{60} and NR- C_{60} systems. The qualitative studies of spatial and temporal trajectories of the admolecule as well as quantitative analysis of its mobility (surface diffusion coefficients, D) were carried out and compared. Figure 1 summarizes the different diffusion regimes of both systems as a

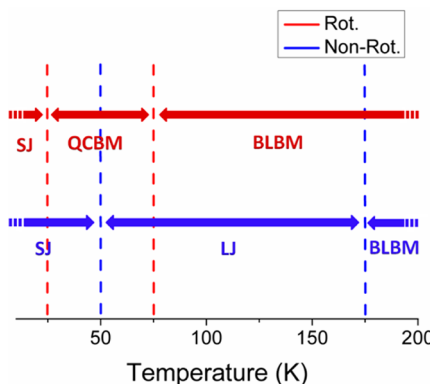


Figure 1. Different regimes of surface diffusion in C_{60} /graphene system according to the effect of temperature and rotational degrees of freedom (DOFs) of the admolecule. In the case of rotational C_{60} (the set of arrows in red), the single jump (SJ) regime dominates below 25 K. Between 25 and 75 K, there is a quasi-continuous Brownian motion (QCBM) regime, which turns into the ballistic-like Brownian motion (BLBM) above 75 K. On the other hand, in the case of nonrotational C_{60} (the set of arrows in blue), the single jump regime (SJ) extends up to 50 K and then turns into the long jump (LJ) regime above 50 K. The LJ regime extends up to 175 K, and finally there is a BLBM regime at elevated temperature similar to the case of rotational C_{60} .

function of temperature. From the upper set of arrows (red color) of Figure 1, it is seen that the R- C_{60} at temperatures below 25 K exhibits the thermally activated hopping motion (stick-slip motion) dominated by single jumps (SJ regime). An increase in temperature leads a transition to Brownian motion (BM) with two distinct regimes: the quasi-continuous Brownian motion (QCBM) between 25 and 75 K and the ballistic-like Brownian motion (BLBM) above 75 K. It is noted that the crossover from thermally activated jump regime to Brownian motion by increasing temperature was theoretically predicted.¹² In reality,

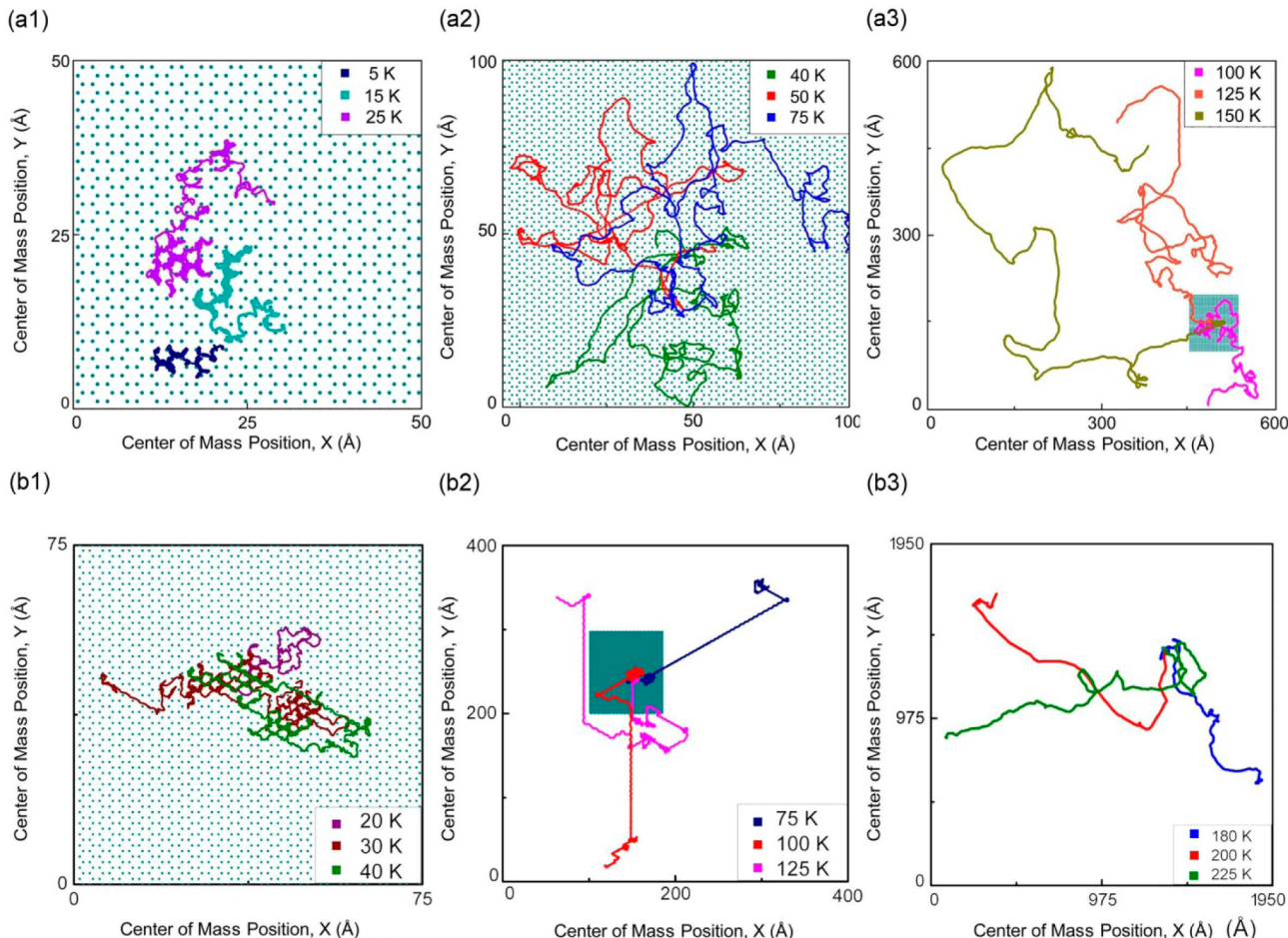


Figure 2. Typical trajectories of C_{60} admolecule on graphene illustrate various surface diffusion regimes in the system at different conditions: (a) in the present of rotational DOFs (a1: SJ; a2: QCBM; a3: BLBM), and (b) in the absence of rotational DOFs (b1: SJ; b2: LJ; b3: BLBM).

however, observation of an adsorbate undergoing Brownian motion is relatively rare,⁴⁵ and the existence of these two distinct regimes of Brownian surface diffusion in the R- C_{60} /graphene system was just recently reported.³³ The lower set of arrows (blue color) in Figure 1 shows that the NR- C_{60} exhibits the SJ motion with temperatures up to 50 K. At temperatures between 50 and 175 K, the NR- C_{60} still performs stick-slip motion; however, its dynamics is dominated by frequent occurrence of very long jumps (flights). At temperatures above 175 K, the NR- C_{60} also undergoes the BLBM regime. Clearly, the rotational DOFs are able to alter the regimes of surface diffusion. In the following, we present our qualitative and quantitative analyses of these diffusive regimes.

To qualitatively demonstrate the diffusive regimes of C_{60} admolecule appearing in Figure 1, we plot the spatial (x - y) trajectories (4 ns) for each regime in Figure 2. This figure presents the trajectories of R- C_{60} and NR- C_{60} in top and bottom rows ((a) and (b) series), respectively. In the case of R- C_{60} (Figure 2a series), it is seen that the single jump (SJ) motion is dominant at low temperature of 5 K (Figure 2a1). With increasing temperature, multiple jumps gradually kick in. It is well-known that in the thermally activated jump regime, trajectories of an admolecule might be correlated with the profile of the PES of the system.^{12,46} Above 25 K (Figure 2a2), the C_{60} admolecule no longer performs random hopping; rather, it moves continuously at temperatures up to 75 K, and its trajectory is consistent with quasi-continuous Brownian motion

(QCBM regime), similar to that observed in the benzene/graphite system.⁴⁵ With further increasing temperature above 75 K (Figure 2a3), the trajectories follow a ballistic-like Brownian motion (BLBM). A comparison between Figures 2a2 and 2a3 implies that in the QCBM and BLBM regimes the trajectories of R- C_{60} admolecule resemble a Brownian motion in high friction (high viscosity) and low friction (low viscosity) regime, respectively.¹¹

According to Figure 2b1, for NR- C_{60} at low temperatures below 50 K, the admolecule exhibits thermally activated hopping mechanism dominated by single jumps. Increasing the temperature leads to increasing the length of random jumps. Figure 2b2 shows the typical trajectories of NR- C_{60} in the LJ regime. Comparing Figures 2b1 and 2b2 reveals that the anisotropic stick-slip motion, i.e., thermally activated jumps in certain crystallographic directions, is a common feature of the trajectories in the SJ and LJ regimes for NR- C_{60} . However, once the NR- C_{60} in the LJ regime (at intermediate temperatures) acquires enough translational energy toward a specific direction, it performs relatively very long jumps (flights) in comparison with the lattice parameter of the graphene. A visual inspection of trajectories in Figure 2b2 reveals that the stick-slip motion of NR- C_{60} in LJ regime resembles a Lévy flight⁴⁷ pattern of diffusion. A similar Lévy flight pattern was also reported in a few other systems, such as gold-cluster/graphite and graphene-flakes/graphene.^{48–50} Figure 2b3 presents the typical trajectories

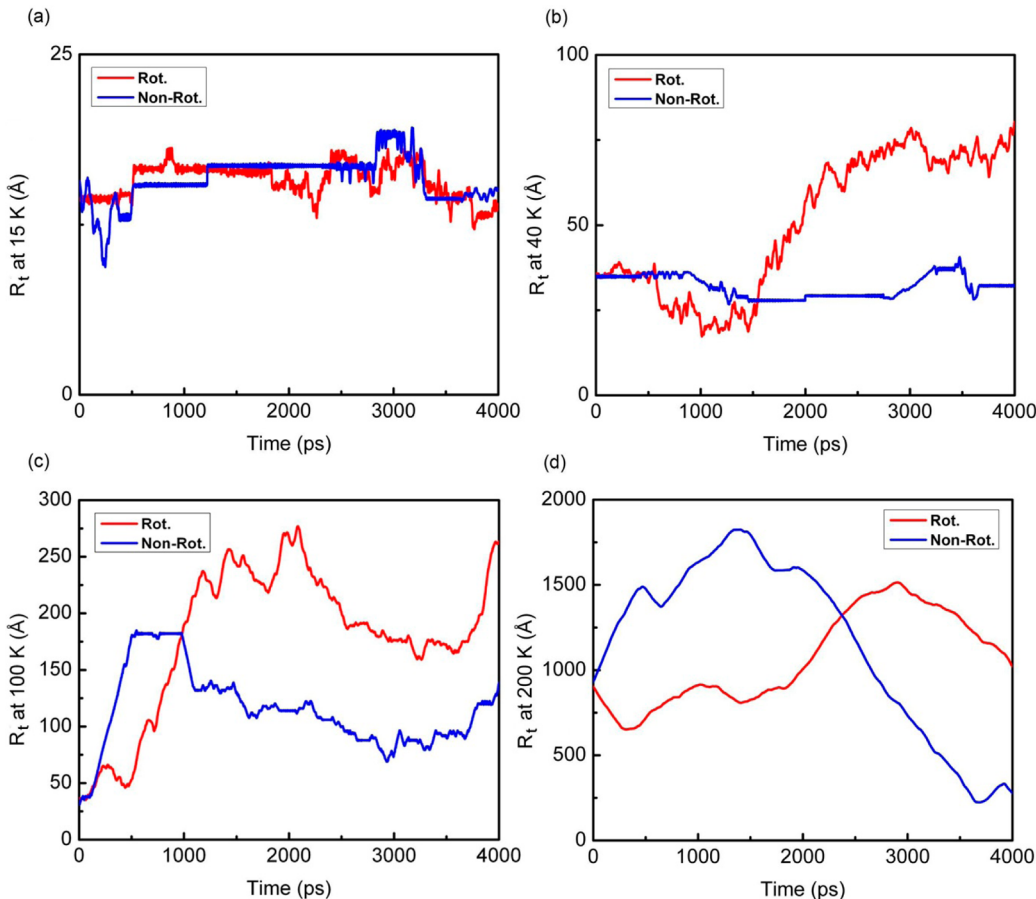


Figure 3. Temporal evolution of the position of C_{60} COM, R , in the presence (red curves) and absence (blue curves) of rotational DOFs at different temperatures: (a) 15, (b) 40, (c) 100, and (d) 200 K. (a) At very low temperature of 15 K, the C_{60} molecule exhibits a stick–slip (hopping) pattern of motion (the sticking intervals separated by jump events) even in the presence of rotational DOFs. (b) At 40 K, in the absence of rotational DOFs, the C_{60} admolecule still moves by hopping mechanism (dominated by single jumps). However, in the case of rotational admolecule, there are no sticking intervals and the molecule performs Brownian motion (QCBM regime). (c) At 100 K, the rotational C_{60} clearly performs a Brownian motion, where in the absence of rotational DOFs, it still exhibits stick–slip motion during which very long jumps (flights) are observable. (d) At 200 K, in the presence and absence of rotational DOFs, the C_{60} molecule does not stick to a certain absorption site on the surface, and in both cases it performs a free Brownian motion.

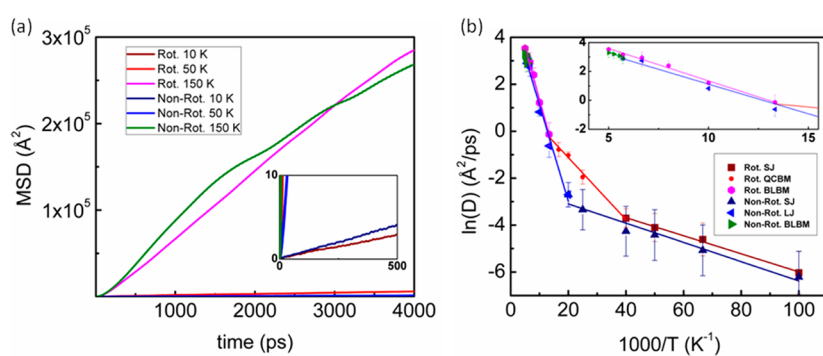


Figure 4. (a) Typical MSD curves at different temperatures. The inset provides a better view of the MSD curves at low temperatures. (b) Effects of temperature and rotational DOFs can be seen on the diffusivity of the C_{60} /graphene system. The Arrhenius analysis of surface diffusion coefficient, D , indicates that in the temperature range of 10–200 K, and in the presence or absence of rotational DOFs, the system undergoes different regimes of surface diffusion. The standard error bars represent the uncertainties in the calculated diffusion coefficients. The inset provides a better resolution of the Arrhenius lines at higher temperatures.

of NR- C_{60} in the BLBM regime (see Figure 1), which is similar to the BLBM in the rotational case.

From Figure 2, it is seen that the trajectory of SJ regime of R- C_{60} (Figure 2a1) is similar to that of NR- C_{60} (Figure 2b1). However, in the absence of rotational DOFs, the SJ regime

extends up to about 50 K. Moreover, in the SJ regime, the trajectories of both R- C_{60} and NR- C_{60} are anisotropic following certain crystallographic pathways on the graphene substrate. Additionally, in the BLBM regime, the trajectories of both R- C_{60} and NR- C_{60} (Figures 2a3 and 2b3, respectively) are alike, since in

both cases, the admolecule moves continuously, similar to a free Brownian particle without confining to any pathway.

To have a clearer qualitative comparison between surface diffusion of C_{60} admolecule in the presence and absence of rotational DOFs, we further analyze the evolution of C_{60} position in time (temporal trajectories), i.e., $R_t = [(x_t)^2 + (y_t)^2]^{1/2}$, where x and y are the coordinates of the C_{60} COM at time t . The variation of R_t in time as shown in Figure 3 is able to reveal the occurrence of trapping in local energy minima and discriminate between stick-slip and Brownian motion. From Figure 3a, it can be seen that at very low temperature of 15 K, the C_{60} molecule exhibits a stick-slip (SJ) motion with localized vibrations at adsorption sites both in the presence and absence of rotational DOFs. The sticking intervals are separated by hopping events. At 40 K (Figure 3b), NR- C_{60} still diffuses by hopping mechanism which is dominated by single/short jumps (SJ regime), whereas R- C_{60} moves almost continuously without trapping at adsorption sites (QCBM regime). At 100 K (Figure 3c), R- C_{60} exhibits continuous BM, whereas NR- C_{60} still exhibits stick-slip diffusion with frequent occurrence of long jumps (similar to Lévy flight). Comparing the R_t curves of NR- C_{60} in Figure 3a–c indicates a crossover in the surface diffusion of NR- C_{60} from the SJ to LJ regime. At 200 K (Figure 3d), the temporal trajectories of R- C_{60} and NR- C_{60} are almost identical and the admolecule undergoes a Brownian motion, corresponding to the BLBM regimes in Figure 1.

The quantitative analysis was also carried out to characterize the diffusive regimes of C_{60} /graphene system for both R- C_{60} and NR- C_{60} . The diffusion coefficient, D , was calculated using the best linear fit to the MSD curves for the temperature range of 10–200 K (typical MSD curves are provided in Figure 4a). The variation of the logarithm of D versus the inverse of the temperature is plotted in Figure 4b for both R- C_{60} and NR- C_{60} . To analyze the temperature dependence of the diffusion coefficient, D , we employed the widely used Arrhenius form consisting of a prefactor, D_0 , and an exponential term as

$$D = D_0 \exp\left(\frac{-E_a}{k_B T}\right) \quad (2)$$

where E_a is the activation energy of the diffusion process. If the adsorbate follows the traditional description of surface diffusion based on the single jump mechanism and the transition state theory (TST) at the entire temperature range, the Arrhenius analysis would offer a perfect linear fit, and the resulting activation energy of diffusion would coincide with the potential energy barrier of the diffusion path.¹¹ However, Figure 4b illustrates that at the studied temperature range the values of D for both R- C_{60} and NR- C_{60} deviate from a single linear fit. Hence, a single value of activation energy cannot be assigned to explain the dynamics of the systems, but rather, D appears to follow several Arrhenius regimes with different activation energies. The corresponding D_0 and E_a values of the Arrhenius regimes and their corresponding temperature ranges are summarized in Table 1.

As can be seen in Figures 2b1 and 2b2, the NR- C_{60} has diffusive pathways parallel to the $\langle 120 \rangle$ crystallographic directions of the graphene substrate. Hence, in order to illuminate the mechanisms of different regimes of surface diffusion for both R- C_{60} and NR- C_{60} , we would like to address a key question: why does NR- C_{60} has a directional pathway (along the $\langle 120 \rangle$ crystallographic direction of graphene substrate) in its SJ and LJ regimes? To answer this question,

Table 1. Arrhenius Parameters of Different Diffusive Regimes and Their Corresponding Temperature Ranges in the Presence and Absence of Admolecule Rotational DOFs (R- C_{60} and NR- C_{60} , Respectively)

system	regime	D_0 ($\text{\AA}^2/\text{ps}$)	E_a (meV)	temp range (K)
R- C_{60} /graphene	SJ	0.12	3.8	<25
	QCBM	4.6	11.3	25–75
	BLBM	330.3	36.4	>75
NR- C_{60} /graphene	SJ	0.14	4.1	<50
	LJ	107.2	29.6	50–175
	BLBM	343.9	37.8	>175

we study the PES of the C_{60} /graphene system since it plays an important role in diffusion dynamics behind the scene of admolecule motion. The most stable configuration of C_{60} , that is, one of its hexagons is oriented parallel to the hexagons of the graphene substrate,^{51,52} was used to calculate the PES of the system. The three-dimensional (3D) PES of the system and its corresponding contour plot are presented in Figures 5a and 5b, respectively. We refer to this configuration as “hexagon in phase” (Hex.-In Phase), and the same configuration was used in diffusion simulations of NR- C_{60} . The PES of the C_{60} /graphene system has a global minimum and maximum when the vertical projection of the C_{60} COM coincides with the center of sp^2 bonds of the graphene carbon atoms and with the geometrical center of the graphene hexagons, respectively. The difference between minimum and maximum values of the potential energy is about 24 meV. This relatively shallow PES is due to the weak van der Waals interactions between the physisorbed C_{60} admolecule and the graphene substrate. In addition, the PES of the C_{60} /graphene system has an interesting feature: there is a pathway parallel to the $\langle 120 \rangle$ crystallographic direction of the graphene (indicated by the vertical blue arrow in Figure 5b), along which there is a minimum-energy barrier of about 4 meV (as illustrated by the potential energy profile in the right inset of Figure 5b). This pathway implies an energetically smooth channel for C_{60} to diffuse on graphene. Note that the energy barrier along the $[100]$ crystallographic direction of the graphene, which is indicated by the horizontal red arrow in Figure 5b, is about 6 times higher than that along the $[120]$ direction (see the corresponding potential energy profile in the top inset of Figure 5b). Hence, one can expect that the trajectories of the NR- C_{60} admolecule should be confined in the diffusion channels parallel to the $\langle 120 \rangle$ family of graphene crystallographic directions. Indeed, this expectation is in good agreement with the directional trajectories of the NR- C_{60} in its SJ and LJ diffusive regimes since they follow the $\langle 120 \rangle$ directions. At elevated temperatures, the NR- C_{60} transits to the BLBM regime (Figure 1) since the thermal energy of the admolecule is comparable with the height of the diffusive channels. Hence, its diffusion should no longer be confined by the profile of the PES of the system, and thus the admolecule performs a free Brownian motion as seen in Figure 2b3.

According to Figures 1 and 2, the R- C_{60} exhibits continuous motion in its QCBM regime, and it is not localized in any adsorption site or confined in a certain pathway, whereas at the same temperature range, the NR- C_{60} exhibits stick-slip motion along the diffusive channels in $\langle 120 \rangle$ direction. To uncover the origin of this difference between the two systems, we consider the effects of C_{60} rotational DOFs together with the finite-size facets on the PES of the system. It was recently shown that when the R- C_{60} admolecule faces an energy barrier on the PES of the system,

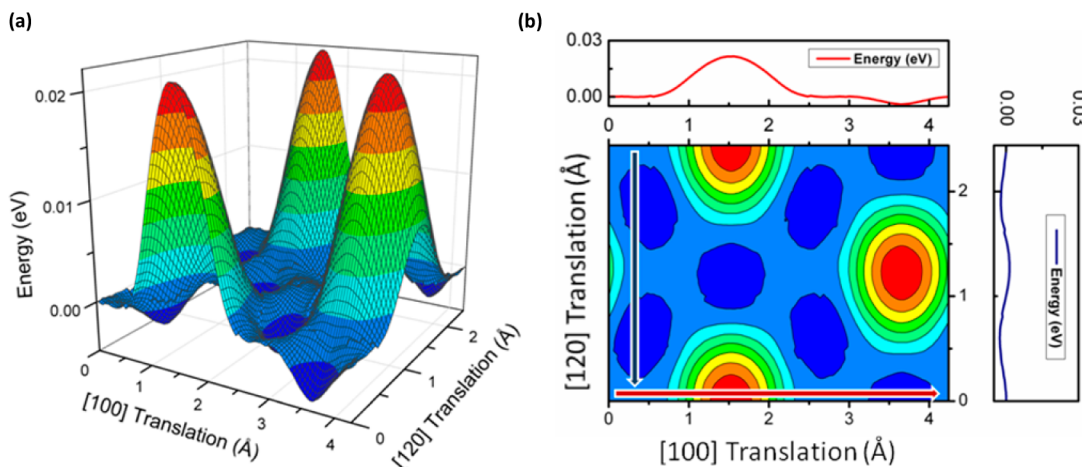


Figure 5. (a) Three-dimensional potential energy surface (PES) of the C₆₀/graphene system for the Hex-In Phase configuration. (b) The corresponding contour plot of the PES. The potential energy profile of the path in the [100] crystallographic direction of graphene (the horizontal red arrow) is plotted on the top inset, while the potential energy profile of the path in the [120] crystallographic direction of graphene (the vertical blue arrow) is plotted on the right inset.

it can overcome the barrier by rotating/tilting to another configuration with a lower energy barrier.³³ Therefore, in the QCBM regime, the rotational DOFs of C₆₀ provide a variety of low-energy pathways for the admolecule to surpass the energy barriers, and consequently, there is no preferable diffusion pathway as the case of NR-C₆₀. However, at elevated temperatures, both R-C₆₀ and NR-C₆₀ undergo BLBM, which is independent of the PES of the system.

The mechanisms described above together with our quantitative analysis of diffusion coefficients for both R-C₆₀ and NR-C₆₀ can be used to explain the overall effect of rotational DOFs on the mobility of C₆₀ admolecule and the temperature range at which this effect is more pronounced. From Figure 4b it can be seen that the diffusion coefficients of both systems (R-C₆₀ and NR-C₆₀) are almost identical in the SJ and BLBM regimes. In the SJ regimes, the activation energy of diffusion for both R-C₆₀ and NR-C₆₀ is about 4 meV. This is in agreement with the dynamics of surface diffusion of the C₆₀ in the SJ regime, which is dominated by hopping between nearest shallow adsorption sites (~4 meV) along the diffusion channels parallel to the ⟨120⟩ crystallographic directions of graphene. As is seen in Figure 4b, the rotational DOFs clearly enhance the mobility of admolecule in the QCBM regime, while in the same temperature range, the NR-C₆₀ still performs stick-slip motion along the confined diffusive channels. Therefore, one can conclude that the role of rotational DOFs is to enhance the mobility of C₆₀ admolecule by helping it to overcome the energy barriers of the PES in the temperature range of QCBM regime (25–75 K).

Nanoscale building blocks such as molecular motors often operate at finite temperatures.^{30,53,54} Clearly at different temperature regimes, the rotational DOFs of an admolecule can have different impacts on the mobility of the admolecule. The present work provides a framework to control the mobility of these nanoscale building blocks. It is known that surface BM is independent of the PES profile of the system, and the dynamics of motion in the Brownian regime is dominated by kinetic friction.^{21,45,46} Hence, there is a natural link between molecular diffusion and kinetic friction force in the Brownian regime. Therefore, the present work provides an opportunity to study the molecular kinetic friction in two different Brownian regimes (QCBM and BLBM).

SUMMARY

We studied the effect of rotational DOFs on the surface diffusion behavior of an admolecule using MD simulations. The C₆₀/graphene was used as a prototypical physisorbed system. We showed that at very low temperature limit, that is, T < 25 K, the dynamics of surface diffusion in both R-C₆₀ and NR-C₆₀ follows the stick-slip motion dominated by jumps between nearest adsorption sites, which is in agreement with the traditional picture of surface diffusion. At elevated temperatures (T > 175 K) both R-C₆₀ and NR-C₆₀ are in the BLBM regime, and their mobility becomes almost identical. The most pronounced effect of rotational DOFs on the surface diffusion of the admolecule appears in the QCBM regime of the R-C₆₀ (at about 25–75 K). In this regime, the rotational DOFs enhance the mobility of C₆₀ by providing alternative routes for the admolecule to overcome the energy barriers of the PES so that it performs nearly continuous Brownian motion on the surface, while in the absence of rotational DOFs, the NR-C₆₀ still performs a confined stick-slip motion in the diffusive channels along the ⟨120⟩ crystallographic directions of the surface. The present work provides physical insights into understanding the effects of rotational DOFs on the molecular mobility and also provides guidelines for future experiments.^{4,55}

AUTHOR INFORMATION

Corresponding Author

*E-mail: zhangyw@ihpc.a-star.edu.sg.

Notes

The authors declare no competing financial interest.

REFERENCES

- (1) Barth, J. V.; Costantini, G.; Kern, K. *Nature* **2005**, *437*, 671.
- (2) Ou, J.; Wang, Y.; Wang, J.; Liu, S.; Li, Z.; Yang, S. *J. Phys. Chem. C* **2011**, *115*, 10080.
- (3) Tahara, K.; Lei, S.; Adisoemoso, J.; De Feyter, S.; Tobe, Y. *Chem. Commun.* **2010**, *46*, 8507.
- (4) Huang, D. M.; Harrowell, P. *J. Phys. Chem. C* **2011**, *115*, 9526.
- (5) Lee, W.-J.; Ju, S.-P.; Chen, H.-C. *J. Phys. Chem. C* **2009**, *113*, 5573.
- (6) Benítez, J. J.; Heredia-Guerrero, J. A.; Serrano, F. M.; Heredia, A. J. *Phys. Chem. C* **2008**, *112*, 16968.
- (7) Raut, J. S.; Fichthorn, K. A. *J. Chem. Phys.* **1998**, *108*, 1626.

- (8) Mahaffy, R.; Bhatia, R.; Garrison, B. *J. Phys. Chem. B* **1997**, *101*, 771.
- (9) Guerra, R.; Tartaglino, U.; Vanossi, A.; Tosatti, E. *Nat. Mater.* **2010**, *9*, 634.
- (10) Browne, W. R.; Feringa, B. L. *Nat. Nanotechnol.* **2006**, *1*, 25.
- (11) Ala-Nissila, T.; Ferrando, R.; Ying, S. C. *Adv. Phys.* **2002**, *51*, 949.
- (12) Ala-Nissila, T.; Ying, S. C. *Phys. Rev. Lett.* **1990**, *65*, 879.
- (13) Liu, Q.; Du, S.; Zhang, Y.; Jiang, N.; Shi, D.; Gao, H.-J. *Small* **2012**, *8*, 795.
- (14) Calvo-Almazán, I.; Miret-Artés, S.; Fouquet, P. *J. Phys.: Condens. Matter* **2012**, *24*, 104007.
- (15) Buchner, F.; Xiao, J.; Zillner, E.; Chen, M.; Röckert, M.; Ditze, S.; Stark, M.; Steinrück, H.-P.; Gottfried, J. M.; Marbach, H. *J. Phys. Chem. C* **2011**, *115*, 24172.
- (16) Maiti, A.; Zepeda-Ruiz, L. A.; Gee, R. H.; Burnham, A. K. *J. Phys. Chem. B* **2007**, *111*, 14290.
- (17) Idrissi, A.; Damay, P.; Krishtal, S.; Kiselev, M. *J. Phys. Chem. B* **2006**, *110*, 18560.
- (18) Dobbs, K. D.; Doren, D. *J. Chem. Phys.* **1992**, *97*, 3722.
- (19) Pai, S.; Doren, D. *Surf. Sci.* **1993**, *291*, 185.
- (20) Dobbs, K. D.; Doren, D. *J. Chem. Phys.* **1993**, *99*, 10041.
- (21) Fouquet, P.; Johnson, M. R.; Hedgeland, H.; Jardine, A. P.; Ellis, J.; Allison, W. *Carbon* **2009**, *47*, 2627.
- (22) de Wijn, A. S. *Phys. Rev. E* **2011**, *84*, 011610.
- (23) Martínez-Galera, A. J.; Gómez-Rodríguez, J. M. *J. Phys. Chem. C* **2011**, *115*, 23036.
- (24) Oyer, A. J.; Carrillo, J.-M. Y.; Hire, C. C.; Schniepp, H. C.; Asandei, A. D.; Dobrynin, A. V.; Adamson, D. H. *J. Am. Chem. Soc.* **2012**, *134*, 5018.
- (25) Hashimoto, A.; Iwao, K.; Tanaka, S.; Yamamoto, A. *Diamond Relat. Mater.* **2008**, *17*, 1622.
- (26) Hashimoto, A.; Terasaki, H.; Yamamoto, A.; Tanaka, S. *Diamond Relat. Mater.* **2009**, *18*, 388.
- (27) Miura, K.; Kamiya, S.; Sasaki, N. *Phys. Rev. Lett.* **2003**, *90*, 055509.
- (28) Harneit, W. *Phys. Rev. A* **2002**, *65*, 032322.
- (29) Naruo, S.; Noriaki, I.; Kouji, M. *J. Phys.: Conf. Ser.* **2007**, *89*, 012001.
- (30) Balzani, V.; Credi, A.; Venturi, M. *ChemPhysChem* **2008**, *9*, 202.
- (31) Simon, F.; Peterlik, H.; Pfeiffer, R.; Bernardi, J.; Kuzmany, H. *Chem. Phys. Lett.* **2007**, *445*, 288.
- (32) Montellano, A.; Da Ros, T.; Bianco, A.; Prato, M. *Nanoscale* **2011**, *3*, 4035.
- (33) Jafary-Zadeh, M.; Reddy, C. D.; Sorkin, V.; Zhang, Y.-W. *Nanoscale Res. Lett.* **2012**, *7*, 148.
- (34) Jafary-Zadeh, M.; Reddy, C. D.; Zhang, Y.-W. *Phys. Chem. Chem. Phys.* **2012**, *14*, 10533.
- (35) Neek-Amal, M.; Abedpour, N.; Rasuli, S. N.; Naji, A.; Ejtehadi, M. R. *Phys. Rev. E* **2010**, *82*, 051605.
- (36) Plimpton, S. *J. Comput. Phys.* **1995**, *117*, 1.
- (37) Brenner, D. W.; Shenderova, O. A.; Harrison, J. A.; Stuart, S. J. *J. Phys.: Condens. Matter* **2002**, *14*, 783.
- (38) Xu, Z.; Buehler, M. *J. ACS Nano* **2010**, *4*, 3869.
- (39) Frenkel, D.; Smit, B.; Ratner, M. A. *Phys. Today* **1997**, *50*, 66.
- (40) Prasad, M.; Sinno, T. *Phys. Rev. B* **2003**, *68*, 045206.
- (41) Jellinek, J.; Beck, T. L.; Berry, R. S. *J. Chem. Phys.* **1986**, *84*, 2783.
- (42) Jellinek, J.; Li, D. *Phys. Rev. Lett.* **1989**, *62*, 241.
- (43) Li, D.; Jellinek, J. *Z. Phys. D: At., Mol. Clusters* **1989**, *12*, 177.
- (44) Aubry, S.; Webb III, E. B.; Wagner, G. J.; Klein, P. A.; Jones, R. E.; Zimmerman, J. A.; Bammann, D. J.; Hoyt, J. J.; Kimmer, C. J. *A Robust Coupled Approach for Atomistic-Continuum Simulation*; Sandia National Laboratories: Albuquerque, NM, 2004.
- (45) Hedgeland, H.; Fouquet, P.; Jardine, A. P.; Alexandrowicz, G.; Allison, W.; Ellis, J. *Nat. Phys.* **2009**, *5*, 561.
- (46) Irene, C.-A.; et al. *J. Phys.: Condens. Matter* **2010**, *22*, 304014.
- (47) Barthelemy, P.; Bertolotti, J.; Wiersma, D. S. *Nature* **2008**, *453*, 495.
- (48) Luedtke, W. D.; Landman, U. *Phys. Rev. Lett.* **1999**, *82*, 3835.
- (49) Maruyama, Y. *Phys. Rev. B* **2004**, *69*, 245408.
- (50) Lebedeva, I. V.; Knizhnik, A. A.; Popov, A. M.; Ershova, O. V.; Lozovik, Y. E.; Potapkin, B. V. *Phys. Rev. B* **2010**, *82*, 155460.
- (51) Gravil, P. A.; Devel, M.; Lambin, P.; Bouju, X.; Girard, C.; Lucas, A. A. *Phys. Rev. B* **1996**, *53*, 1622.
- (52) Legoas, S. B.; Giro, R.; Galvão, D. S. *Chem. Phys. Lett.* **2004**, *386*, 425.
- (53) Gimzewski, J. K.; Joachim, C.; Schlittler, R. R.; Langlais, V.; Tang, H.; Johannsen, I. *Science* **1998**, *281*, 531.
- (54) Porto, M.; Urbakh, M.; Klafter, J. *Phys. Rev. Lett.* **2000**, *84*, 6058.
- (55) Perera, U.; Ample, F.; Kersell, H.; Zhang, Y.; Vives, G.; Echeverria, J.; Grisolia, M.; Rapenne, G.; Joachim, C.; Hla, S. *Nat. Nanotechnol.* **2013**, *8*, 46–51.